Near-Field Character of a Jet Discharged through a Wall at 30° to a Mainstream

G. Bergeles,* A. D. Gosman,† and B. E. Launder‡
Imperial College of Science and Technology, London, England.

Measurements are reported of the flow created by the injection of a circular jet at 30° through a plane wall, past which an external stream is flowing. Attention has been focused on the region immediately surrounding the injection hole, which has received slight attention in earlier studies. The data include profiles of streamwise velocity and distributions of static pressure and film-cooling effectiveness on the surface, for ratios of average injection velocity: freestream velocity M of 0.1, 0.2, 0.5, 1.0, and 1.5. Flow visualization photographs also are presented. Two modes of behavior are observed, according to the magnitude of M. For values of 0.3 and less, the injected jet remains attached to the surface, provoking considerable pressure and velocity disturbances, and giving rise to increasing effectiveness as M is increased. At values of M of 0.5 and above, the jet lifts off the surface, allowing penetration of the mainstream fluid beneath it. As a consequence, the effectiveness now diminishes as M is augmented, as are the surface pressure disturbances, and a complex flow structure is produced. Maximum effectiveness and coverage is observed when M is about 0.5, in conformity with earlier studies.

Nomenclature

c = concentration of tracer gas
C_p = pressure coefficient $[(C_p = (p - p_{ref}) / (\frac{1}{2}\rho_c v_j u_\infty)]$
D = hole diameter
M = blowing rate $(M = \rho_c V_c / \rho_\infty u_\infty)$
p = static pressure
Re_D = Reynolds number $(Re_D = \rho_\infty u_\infty D / \mu_\infty)$
S = hole spacing
u = streamwise velocity component
v = normal velocity component
V = mean resultant injection velocity
x = streamwise direction
x' = streamwise distance from virtual origin of boundary layer
y = direction normal to the surface
z = lateral direction

Greek Symbols

α = angle of injection
δ = boundary-layer thickness
δ_1 = displacement thickness
η = wall film cooling effectiveness
μ = dynamic viscosity
ρ = density

Subscripts

c = coolant
ℓ = center line
j = injection
∞ = freestream
ref = reference point located at $x/D = 2.0$, $y/d = 1.5$, $z/D = 0$

I. Introduction

THE continual rise in turbine inlet temperature projected over the next decade underlines the need for blade materials with better heat-resistance characteristics and/or better methods of cooling the blades. One such method, which is attracting attention, is discrete-hole film cooling, in which low-temperature secondary fluid is supplied via passages within the blade to an array of holes leading to the surface, thereby forming a protective coolant film. As in other film-cooling methods, the extent of the region that is protected by any one coolant source is limited, because of penetration by and mixing with the hot main stream: such systems therefore must be designed with care.

The parameters that govern the effectiveness of discrete-hole cooling are numerous, and include the number, arrangement, and spacing of the holes, the magnitude and angle of injection, the relative densities of the main stream and coolant flows, the prevailing pressure gradient and boundary-layer thickness, etc. Consequently, although many experiments have been conducted into the effects of some of these parameters on the film-cooling effectiveness and/or the flow structure,[1-10] knowledge is by no means sufficiently complete to insure that a designer could identify the best cooling arrangement.

The authors currently are developing an alternative, and potentially more flexible, method of parameter exploration in which computer predictions of the cooling process are obtained by numerical solution of the governing differential equations.[11-12] Studies made with the method have shown that the adequacy of the predictions depends crucially on the correct calculation of the flow in the immediate vicinity of the holes, a region that unfortunately has received little attention in the majority of the experiments cited previously. Accordingly, a program of measurements was undertaken, aimed specifically at providing detailed information about this region, to be used to validate and improve the prediction method. Some of the data obtained already have been reported in Ref. 13, which is concerned with 90° injection through a single hole. In the present paper, we report measurements for 30° injection through a single hole, for conditions of uniform-density flow with zero pressure gradient. The data include distributions of streamwise velocity, film-cooling effectiveness, and wall static pressure: these are complemented by visualization studies, which help to reveal the character of the flow.

II. Apparatus and Measurement Technique

A. Apparatus

The experiments were performed in the same wind tunnel and test section as those of Ref. 13, except that an entirely new plexiglass test plate was fabricated. As indicated in Fig. 1, secondary air was admitted through a tube of 19.05-mm

Received May 24, 1976; revision received Sept 24, 1976.
Index category: Boundary Layers and Convective Heat Transfer—Turbulent.

*Research Assistant, Mechanical Engineering Department.
†Lecturer, Mechanical Engineering Department.
‡Reader, Mechanical Engineering Depart.

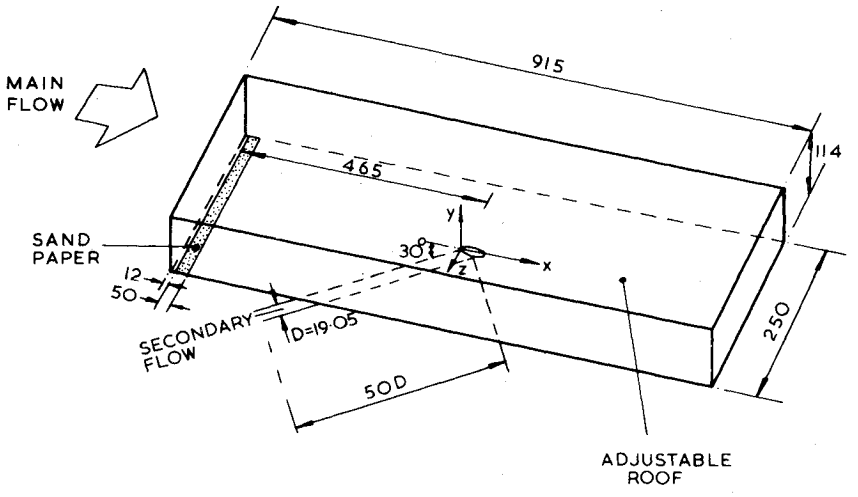

Fig. 1 Diagram of test section. Dimensions in mm.

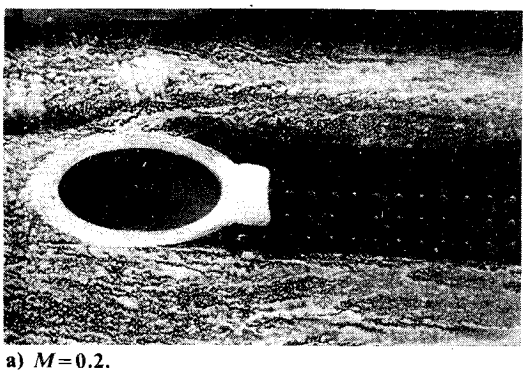

a) $M=0.2$.

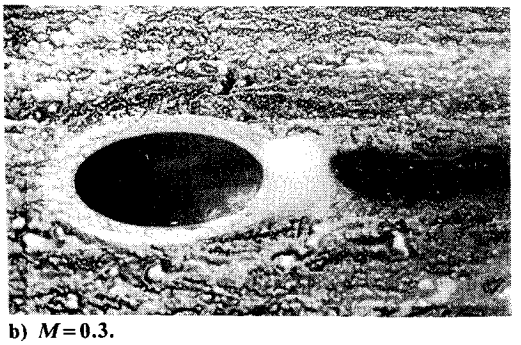

b) $M=0.3$.

Fig. 2 Surface streamline pattern.

internal diam, which was set at 30° to the plate surface with axis pointing downstream: the secondary flow rate was measured with a calibrated orifice plate. The surface of the plate around the injection hole was drilled with an array of static pressure tappings 0.79-mm in diam: the precise locations of the holes are shown in Fig. 3a, cited later in this report.

The instrumentation and measurement techniques were the same as those for the previous study.[13] The estimated uncertainty levels in the measurements also are comparable: maximum errors in velocity measurements with a pitot static probe due to uncertainties in flow angle and high turbulence level are estimated at 2%, except immediately downstream of the hole, where the strong disturbance caused by injection gives rise to indeterminate errors. The values of film cooling effectiveness (obtained by measuring at the plate surface the concentration of a tracer of helium introduced into the secondary air supply) are estimated to be accurate to within 5% throughout.

The experiments were carried out for a fixed freestream velocity of 26 m/sec, and values of the injection: freestream velocity ratio M of 0.1, 0.2, 0.3, 0.5, 1.0, and 1.5. Further, in order to define the flow conditions adequately, measurements also were taken without secondary injection, with the hole covered. The recorded velocity profiles at various lateral locations along a plane passing through the upstream edge of the hole and closely obey the relation $u/u_\infty = (y/\delta)^{1/6.5}$. The virtual origin of the boundary layer is located approximately 32.5 hole diam from the upstream edge of the hole. The inferred nondimensional displacement thickness variation was found to be uniform across the tunnel to within 0.2% and to have the value 0.122 D at the position corresponding to the leading edge of the hole: the corresponding displacement-thickness Reynolds number was 4030. Table 1 summarizes the range of conditions of the present measurements and those of some of the earlier studies with which comparisons will be made.

III. Presentation of Results

A. Flow Visualization

First, we will examine some qualitative information about the flow obtained by spreading over the test plate upstream of the hole a mixture of yellow pigment and kerosene, and then turning on the air supplies. The photograph in Fig. 2a reveals, for $M=0.2$, the surface "streamline" pattern, which emerges when the liquid spreads and then evaporates, leaving the yellow pigment. Evidently, the upstream flow scarcely is affected by the injection (presumably because the jet is directed downstream: when the injection angle is 90°, appreciable upstream effects are observed[13]) whereas downstream there exists a clear region in which jet remains substantially attached to the surface. Figure 2b shows the pattern for $M=0.3$: the behavior is similar, but the lateral extent of

Table 1 Summary of experimental conditions of relevant studies

Reference	Geometry	α	δ_1/D	S/D	ρ_c/ρ_∞	Re_D	M
Present	Single hole	30°	0.122	∞	1.0	3.3×10^4	0.1-1.5
(5)	Single hole	35°	0.051	∞	0.85	8.7×10^4	0.1-1.0
(7)	Row of holes	35°	0.156	3.0	1.06	2.0×10^4	0.2-1.5
(15)	Single hole	35°	0.116	∞	0.85	4.4×10^4	0.5, 0.75, 1.0
(15)	Single hole	35°	0.124	∞	0.85	2.2×10^4	0.5, 0.75, 1.0
(16)	Row of holes	35°	0.149	3.0	0.85	4.4×10^4	0.2, 0.50, 1.0

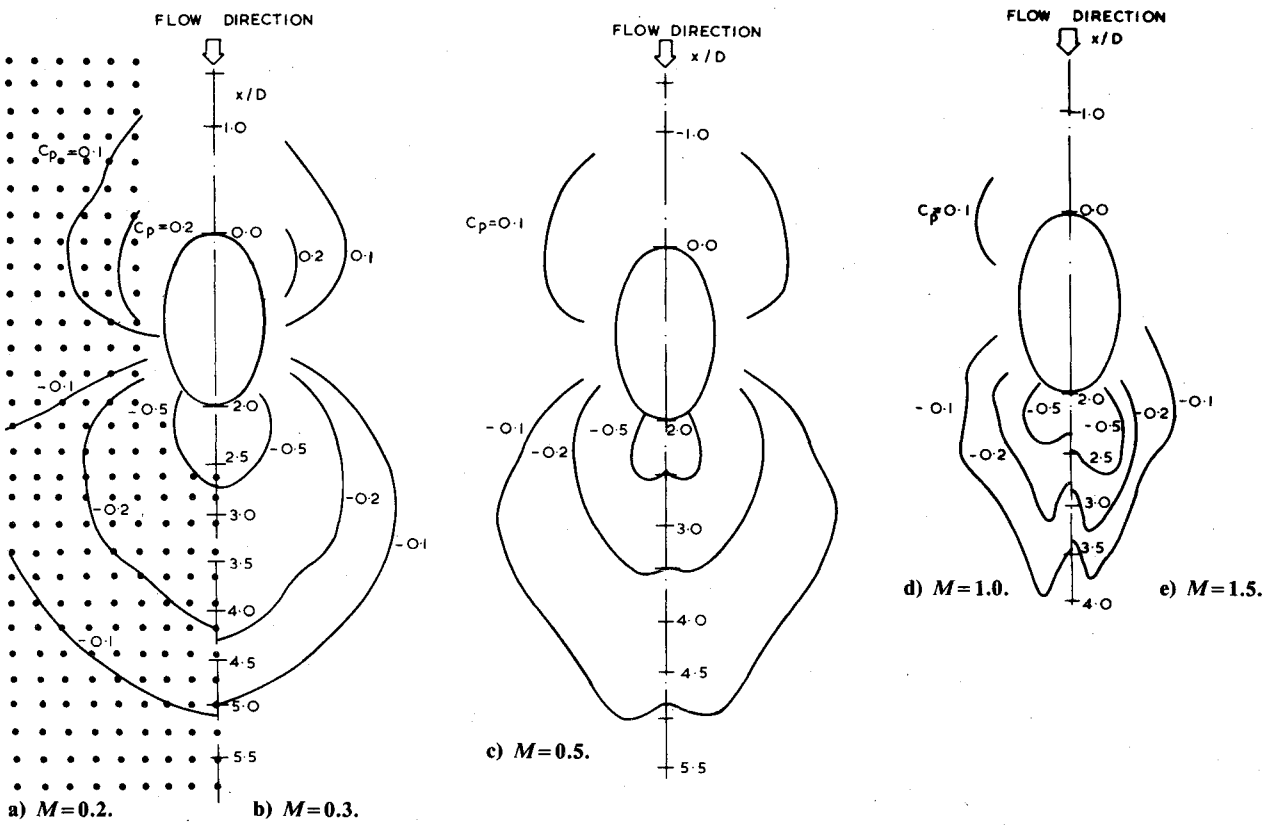

Fig. 3 Surface isobaric contours.

the uncovered region has diminished, because although the jet is still attached to the surface, it is about to lift off. In light of this behavior, it is not surprising that the flow visualization photographs for $M=0.5$ and greater (not shown) reveal total coverage of the surface by the pigment, indicating that the jet has lifted off.

Similar tests with a tracer fluid introduced at varying distances *downstream* of the hole indicate the presence, for all M, of a small zone of recirculation attached to the downstream edge of the hole and of approximate dimensions 0.5 D wide and 0.3 D in length,§ which was fed by upstream air entering from the sides. The extent of the recirculation was far smaller than that observed in Ref. 13 for normal injection at comparable M. Some quantitative information about these and other facets of the flow behavior on the velocity, pressure, and concentration fields now will be given.

B. Wall Static Pressure

Figures 3a–3e show the distributions of static pressure in the vicinity of the hole for various values of injection ratio M in the range 0.2–1.0, plotted as contours of the pressure coefficient c_p, which is defined as

$$c_p \equiv (p - p_{\text{ref}}) / \tfrac{1}{2}\rho_c u_\infty v_j$$

where p is the local pressure, and p_{ref} is its value in the undisturbed region far upstream of the hole.

Certain features are common to all plots: thus, there is a region of positive pressure starting some distance along the hole and extending laterally and upstream; the distribution suggests that the peak value of c_p occurs near the leading edge of the hole. Proceeding downstream from this region, the pressure rapidly falls to a minimum negative value near the downstream end of the hole and recovers thereafter. The zone of negative c_p also extends laterally, and its total extent

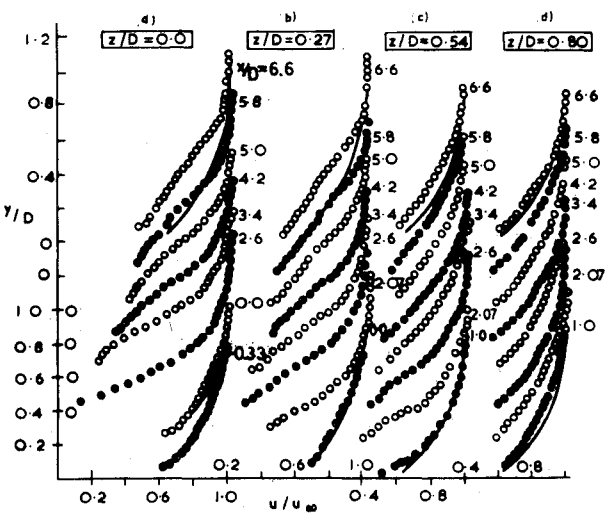

Fig. 4 Profiles of the streamwise velocity for $M=0.2$

generally is greater than the upstream one, if we take the $|c_p|=0.1$ contour as a measure. This behavior may be explained, as in Ref. 13, by regarding the jet as an 'obstacle' attached to the surface which obstructs the upstream flow, causing the pressure there to rise; the level of c_p then falls, becoming negative as the deflected fluid accelerates around the hole. Eventually in the downstream region there is a gradual recovery of pressure as the flow reverts back to a normal boundary layer.

Of course the present 'obstacle' is a rather special one, whose shape and other characteristics are functions of the injection rate: for example, the emerging jet shears the mainstream flow in a direction opposed to the sense of rotation of a vortex created by the bending of the boundary-layer vorticity lines around a blunt object. Therefore, it is not surprising that the surface pressure distribution turns out to

§These dimensions are not those of the pigment-covered region in the photograph just downstream of the hole, for the build-up of pigment fluid has exaggerated the apparent size of the zone.

be a function of M. It is, however, interesting to note that, for the two lower blowing rates, the distributions are quite similar when scaled by $\rho_c u_\infty v_j$; this seems to be a general characteristic of discrete jets when they remain substantially attached to the surface, because similar behavior was observed in our earlier 90° study for $M=0.1$ and 0.24. It is presumably connected with the fact that $\rho_c v_j u_\infty$ is proportional to the streamwise momentum deficit of the injected fluid.

C. Streamwise Velocity Distribution

The next series of figures displays the development of the streamwise velocity on the center, and in some cases off-center, planes. Typical of the results for the low injection ratios are the data in Fig. 4 for $M=0.2$ (the solid line in this and the remaining figures is the velocity profile that would prevail in the absence of injection, provided for comparison). Referring to the center-plane development in Fig. 4a, we see that the upstream flow at $x/D=-0.33$ and 0 is mildly retarded by the adverse pressure gradient, whereas immediately downstream of the hole, at $x/D=2.60$, the slow-moving near-wall fluid is that which has just emerged from the injection hole.¶ Further downstream the action of shear stresses causes the momentum of this fluid to increase (at the expense of that of the surrounding fluid) despite the prevailing adverse pressure gradient. Figures 4b–4d reveal similar, but diminishing effects on planes increasingly remote from the center, because of the smaller amounts of injected fluid which are present there. The disturbance barely extends to the plane at $z/D=0.8$, which is beyond the edge of the hole. As M is increased to 0.3, only slight differences are observed, as is shown in Fig. 5.

Not surprisingly, the streamwise velocity distributions for $M=0.5$, 1.0, and 1.5 (Figs. 6–8) are different from those for lower M, because of lift-off-phenomenon (although those for $M=0.5$ share some features with both groups and could therefore be regarded as representing a transitional state); however, within themselves they again exhibit strong similarities. Figure 7 for $M=1.0$ is representative of this group, revealing insignificant upstream effects (because the injection velocity is very nearly that of the boundary layer) and a rather complex downstream structure. Initially it consists of three distinct regions identified as the disturbed outer portion of the boundary layer, the detached jet (signaled first at $x/D=2.33$ by the presence of the inner maximum in the velocity profile), and the layer of near-wall fluid beneath the jet. It is interesting to note that, although the layer underneath the jet is initially retarded (presumably for the same reasons as at lower M), it subsequently appears to "accelerate" beyond the velocity of the jet, thereby producing another maximum (see $x/D=2.60$ et seq). The reason for this is not obvious (recall that the near-wall pressure gradient is small and in any case adverse) but it may be because of the action of the familiar counter-rotating vortices known to exist in such flows[12] bringing in high velocity fluid from outer layers.** Eventually the layers merge, but the profiles remain far from the undisturbed one even at the furthest downstream station. At off-center planes, the three-layer structure initially persists ($z/D=0.27$), and then reverts to a simpler pattern. The disturbances essentially have disappeared by $z/D=0.8$ (not shown).

The center plane profiles for $M=0.5$ (Fig. 6) and 1.5 (Fig. 8) differ from the preceding profiles only in minor respects: for example, in the latter case, the streamwise velocity of the injected fluid is greater than the freestream velocity of the boundary layer; hence the occurrence of the maximum velocity within the layer.

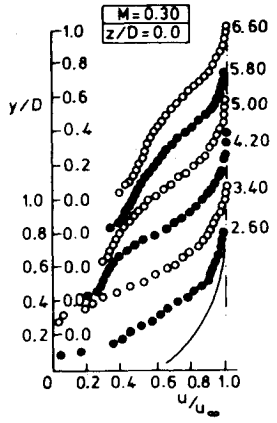

Fig. 5 Profiles of the streamwise velocity on symmetry plane, $M=0.3$.

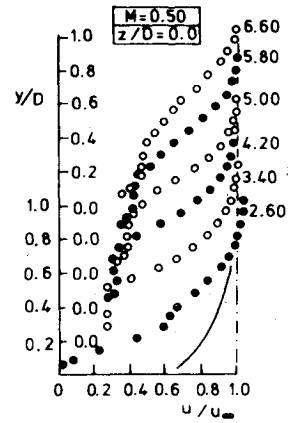

Fig. 6 Profiles of the streamwise velocity on symmetry plane, $M=0.5$.

D. Wall Film Cooling Effectiveness Measurements

Measured distributions of film-cooling effectiveness are shown for different blowing rates in Figs. 9a–9f. The effectiveness is plotted against the downstream distance (x/D) at various lateral locations.†† The general trend at the two lower blowing rates $M=0.1$ and 0.2 (Figs. 9a and 9b, respectively) is for the effectiveness to decay along lines passing through the hole, and to rise and fall along lines passing nearby: both effects are caused by the spreading of the jet amd mixing with the mainstream fluid (including that entering the recirculation zone behind the hole). Comparison of the two figures reveals that, at this level of blowing, the effect of increasing M is to increase the level and extent of coverage.

Also shown in the previously mentioned plots are data drawn from other sources[5,16] for conditions similar to, but not identical with, the present experiments (cf Table 1). The small discrepancies that are observed may be plausibly attributed to these differences: for example, the tendancy for the data of Ref. 5 to lie above the present measurements in Fig. 9a probably is due to the lower density ratio and displacement thickness of the former, since in Refs. 7‡‡ and 16, it is shown that η_ℓ increases with a reduction in either of these parameters.

The results in Fig. 9c for $M=0.3$ seem at first sight to be similar to those for the lower blowing ratios, but closer inspection reveals the existence of small maxima near the hole for $z/d=0.0$, 0.27. Presumably these are a consequence of increased entrainment into the recirculation zone, coupled with the partial lifting off of the jet, which allows more extensive mixing with the mainstream fluid. The maxima may

¶For the present injection angle, the streamwise velocity of the injected fluid is about $0.9\,Mu_\infty$.

**This argument is reinforced by the observation that the peak velocity measured in this region occurs off-center, at $z/D=0.27$.

††The positions of some of these, it should be noted, shifts between $x/D=6.5$ and 8, due to constraints in the construction of the apparatus.

‡‡These data pertain to a row of holes, but the spacing: diameter ratio was sufficiently large (3:1) that adjacent jets would not be expected to interact in the region examined here.

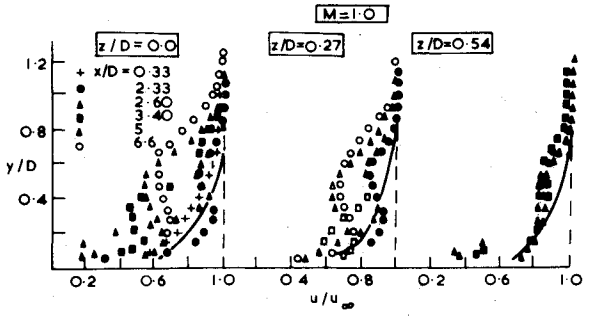

Fig. 7 Profiles of streamwise velocity, $M=1.0$.

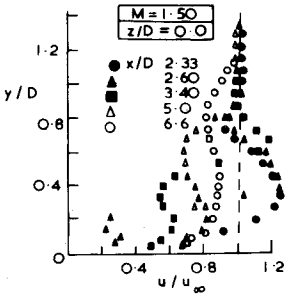

Fig. 8 Profiles of the streamwise velocity on symmetry plane, $M=1.5$.

be regarded as defining the points at which the spreading of the jet has allowed it to 'reattach' to the surface; but it must be emphasized that, in this instance, the 'reattachment' line does not delineate the zone of recirculation. The level and extent of coverage has continued to increase.

As the blowing rate is raised further to $M=0.5$ and beyond, the average level of effectiveness goes through a maximum at $M=0.5$ and then falls, whereas for the higher blowing rates the local maxima in the profiles become more pronounced and shift downstream. This behavior is, of course, the result of the ever-increasing length of the jet trajectory before it reattaches and the consequent dilution of the region beneath by the mainstream fluid. It also is noticeable that, even at $M=0.50$, the off-center values of η are, in some regions, equal to or slightly smaller than those for $M=0.3$, indicating that the lateral spread of the jet is no longer increasing: this is caused by the smaller relative velocity between the jet and adjacent fluid, resulting in reduced mixing.

Figures 9d-9f also contain data from other sources, namely, Refs. 5, 7, 15, and 16. The agreement with the present measurements generally is good, the discrepancies being attributable to differences in experimental conditions, notably the upstream boundary-layer thickness and the density ratio. In particular, it should be noted that the effect of the former parameter diminishes as M increases,which is in conformity with the findings of the Minnesota group.[4-7, 15,16]

IV. Practical Implications

The practical implications of the present study are, perhaps, best perceived from Figs. 10 and 11, where the data for all blowing rates have been assembled. Figure 10 contains the data for the centerline effectiveness, which suggest, in agreement with earlier studies,[15-17] the existence of an optimum value of M of about 0.5 (this assessment only applies, of course, to the particular values of pressure gradient, boundary-layer thickness, etc., employed in those studies). Figure 11 shows that this value also yields the maximum lateral coverage, as measured by the paths of the contours of 20% effectiveness. Further, the width of the 20% region is about 1.4 hole diam, suggesting that the maximum effective spacing between holes should not exceed about 1.4 D if total coverage is to be achieved.

V. Conclusions

1) The injection process gives rise to appreciable disturbances to the flowfield at all injection rates, but, in contrast

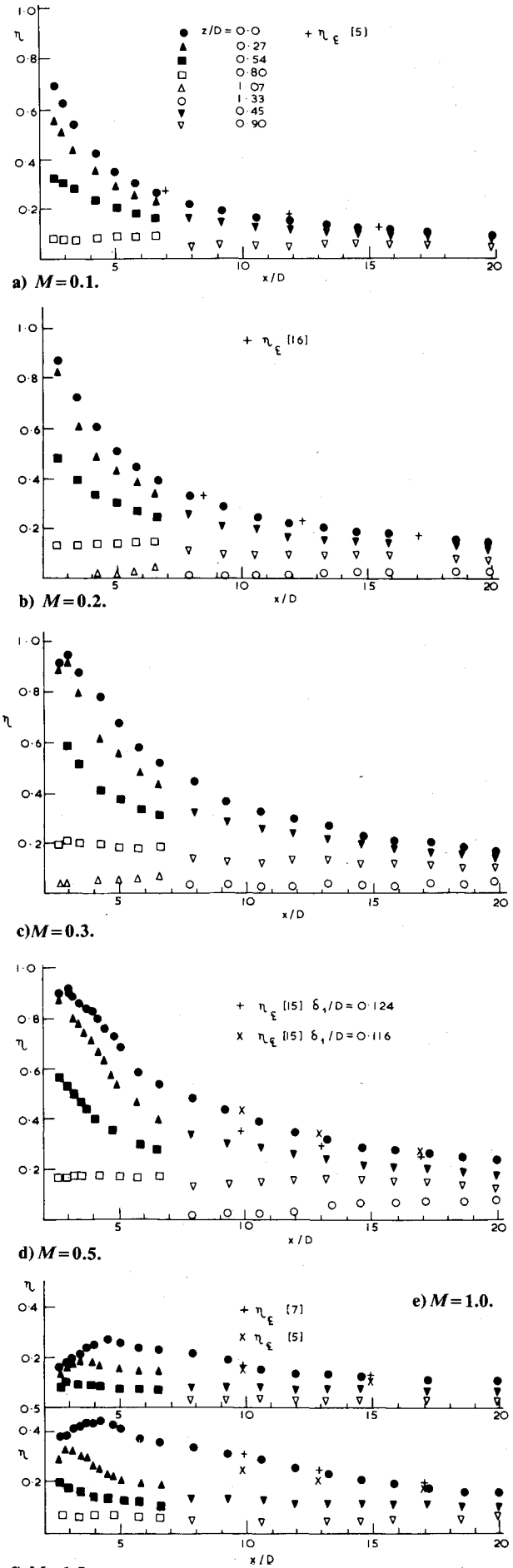

Fig. 9 Wall film-cooling effectiveness.

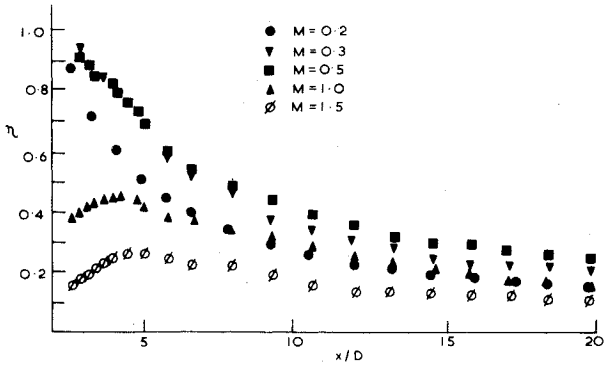

Fig. 10 Effect of M on centerline film-cooling effectiveness.

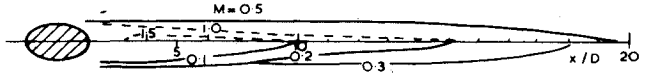

Fig. 11 Effect of M on surface contours of 20% effectiveness.

with 90° injection, the effects are mainly downstream of the hole. Important features of these disturbances are large lateral variations in the streamwise pressure gradient and streamwise recirculation, which are not allowed in conventional analytical and numerical methods of boundary-layer analysis.

2) Two modes of behavior are observed, according to the magnitude of M. For values of about 0.3 and less, the injected jet remains essentially attached to the surface, producing strong surface pressure disturbances, which are proportional to the momentum deficit of the injected fluid; these are characterized by the quantity $\frac{1}{2}\rho_c v_j u_\infty$, and yield effectiveness values that rise when M is increased.

3) When M is about 0.5 or above, the jet completely lifts off the surface, allowing penetration of the mainstream fluid beneath. The length of the trajectory goes up with M. As a consequence, the effectivness now decreases with increasing M, the surface pressure tends to become more uniform, and a complex flow structure is produced downstream of the hole.

4) The present results are in good agreement with measurements from other sources and, in conformity with earlier findings, suggest that for the particular conditions of the measurements the optimum injection rate is about 0.5.

Acknowledgments

We gratefully acknowledge the support of this work by the Ministry of Defense, Procurement Executive.

References

[1]Launcer, B. E. and York, J., "Discrete-Hole Cooling in the Presence of Free-Stream Turbulence and Strong Favorable Pressure Gradient," *International Journal of Heat Mass Transfer*, Vol. 17, 1974, pp. 1430–1409.

[2]Le Brocq, P. V., Launder, B. E., and Priddin, C. H., "Discrete Hole Injection as a Means of Transpiration Cooling; an Experimental Study," *Proceedings of Institution of Mechanical Engineers*, Vol. 187, 1973.

[3]Goldstein, R. J., Eckert, E. R. G., and Burggraf, F., "Effects of Hole Geometry and Density on Three-Dimensional Film Cooling," *International Journal of Heat Mass Transfer*, Vol. 17, 1974, pp. 595–607.

[4]Ramsey, J. W. and Goldstein, R. J., "Interaction of a Heated Jet with a Deflecting Stream," NASA CR-72613, 1968.

[5]Goldstein, R. J., Eckert, E. R. G., and Ramsey, J. W., "Film Cooling with Injection Through Holes: Adiabatic Wall Temperatures Downstream of a Circular Tube," *Transaction of the ASME, Engineering for Power,*, Oct. 1968, pp. 384–395.

[6]Goldstein, R. J., Eckert, E. R. G., Eriksen, V. L., and Ramsey, J. W., "Film Cooling Following Injection Through Inclined Circular Tubes," *Israel Journal of Technology*, Vol. 8, 1970, pp. 145–154.

[7]Pedersen, D. R., "Effect of Density Ratio on Film Cooling Effectiveness for Injection Through a Row of Holes and for a Porous Slot," Ph.D. Thesis, University of Minnesota, Mechanical Engineering Dept., 1972.

[8]Smith, M. R., Jones, T. V., and Schultz, D. L., "Film Cooling Effectiveness from Rows of Holes under Simulated Gas Turbine Conditions," ARC, CP, No. 1303, 1973.

[9]Liess, C., "Experimental Investigation of Film Cooling with Ejection from a Row of Holes for the Application to Gas Turbine Blades," American Society of Mechanical Engineers, Paper 74-9T-5, 1974.

[10]Liess, C. and Carnel, J. "Application of Film Cooling to Gas-Turbine Blades," *AGARD Conference Proceedings, No. 73, on High Temperature Turbines*, 1971.

[11]Bergeles, G., Gosman, A. D., and Launder, B. E., "The Prediction of Discrete-Hole Cooling: A Progress Report on Experience with Parabolic and Partially Versions of STABL," Imperial College, Mechanical Engineering Department Report, 1974.

[12]Bergeles, G., Gosman, A. D., and Launder, B. E., "The Prediction of Three-Dimensional Discrete-Hole Cooling Processes: 1-Laminar Flow," ASME Winter Annual Meeting, 75-WA/HT-109, Dec. 1975.

[13]Bergeles, G., Gosman, A. D., and Launder, B. E., "The Near-Field Character of a Jet Discharged Through a Wall at 90° to a Main Stream," ASME Winter Annual Meeting, 75-WA/HT-108, Dec. 1975.

[14]Baker, R. J. and Launder, B. E., "The Turbulent Boundary Layer with Foreign Gas Injection-1. Measurement in Zero Pressure Gradient," *International Journal of Heat Mass Transfer*, Feb. 1974, pp.275–291.

[15]Goldstein, R. J., Eckert, E. R. G., Eriksen, V. L. and Ramsey, J. W., "Film Cooling Following Injection through Inclined Circular Tubes," NASA CR-72612, Nov. 1969.

[16]Eriksen, V. L., "Film Cooling Effectiveness and Heat Transfer with Injection Through Holes," Ph.D. Thesis, University of Minnesota, Mechanical Engineering Department, 1971.